Available online at www.sciencedirect.com

ScienceDirect

Energy Procedia 45 (2014) 769 – 778

Energy Procedia

68th Conference of the Italian Thermal Machines Engineering Association, ATI2013

A methodology to improve knock tendency prediction in high performance engines

Stefano Fontanesi[a]*, Giuseppe Cicalese[a], Alessandro d'Adamo[a], Giuseppe Cantore[a]

Department of Engineering "Enzo Ferrari", University of Modena and Reggio Emilia, Modena, Italy

Abstract

The paper presents a comprehensive numerical methodology for the estimation of knock tendency in SI engines, based on the synergic use of different frameworks [1]. 3D-CFD in-cylinder analyses are used to simulate the combustion and to estimate the point-wise heat flux acting on engine components. The resulting heat fluxes are used in a conjugate heat transfer model in order to reconstruct the actual point-wise wall temperature distribution. An iterative loop is established between the two simulation realms. In order to evaluate the effect of temperature on knock, in-cylinder analyses are integrated with an accurate chemical description of the actual fuel.

© 2013 The Authors. Published by Elsevier Ltd. Open access under CC BY-NC-ND license.
Selection and peer-review under responsibility of ATI NAZIONALE

"Keywords:Conjugate Heat Transfer, Knock, Heat Transfer, Combustion"

1. Introduction

The brake specific power of internal combustion engines, i.e. the power per displacement unit, is progressively increasing during the last 10 years. On the passenger car engine side, this is especially done through the use of the downsizing technique, which in turn mainly relies on the matching of a turbocharger to a reduced displacement engine; lower fuel consumption and pollutant emissions can be achieved without a substantial reduction of the engine performance [2]. On the high performance engine side, instead, the downsizing is a more recent approach, mainly because of the loss of appeal that could derive from the displacement reduction for the specific market. As a consequence, the need to increase the engine performance while complying with the progressively more stringent

* Corresponding author. Tel.: +39-059-2056114; fax: +39-059-2056126.
E-mail address: stefano.fontanesi@unimore.it

1876-6102 © 2013 The Authors. Published by Elsevier Ltd. Open access under CC BY-NC-ND license.
Selection and peer-review under responsibility of ATI NAZIONALE
doi:10.1016/j.egypro.2014.01.082

pollutant regulations is usually reached through the adoption of variable valve timing controls, variable length ports and gasoline direct injection.

For both engine classes, heat removal from the most stressed components plays a primary role both to avoid mechanical failures and to prevent the arise of abnormal combustions such as knock and/or surface ignition. The formers are in fact mainly due to the reduction of the material strength at high temperature, while the latters can be promoted by local temperature peaks within the unburnt mixture and/or on the walls facing the combustion chamber. This motivates the need to properly design the coolant circuit, which should be able to act over all the most thermally charged components in order to maximize the specific engine performance. For example, the effectiveness of the heat removal has a direct consequence on both the location of the spark advance and the boost pressure level, which in turn are responsible for the optimal location (timing) and magnitude of the in-cylinder pressure trace, and therefore for the amount of indicated work.

On the other side, however, an oversized coolant circuit reduces the thermodynamic efficiency of the engine and is responsible for increased pollutant emission, especially on the unburnt side due to the larger flame quenching thickness.

The accurate evaluation of the thermal field of the engine components under actual engine operations is something far beyond the possibility within the research and development industrial practice, and it is far from being a well-established practice even in highly-specialized research laboratories.

First of all, a relevant number of thermocouples should be distributed among the many components facing the combustion chamber in order to gain a comprehensive characterization of the thermal field within the engine. Then, despite the extremely high thermal gradients close to the combustion chamber would require sensors to be placed as close as possible to the gas-exposed surface, information are available at least a few millimeters within the components, in order to preserve the engine thermo-mechanical strength. Thermal gradients and surface temperatures can only be inferred by placing secondary thermocouples a few millimeters from the primary ones in the wall-orthogonal direction. Finally, thermocouples are usually placed only in the steady components, i.e. the engine head and block, while temperature measurements for the remaining ones (piston, valves, cylinder liners) can only be extrapolated from a-posteriori measurements such as residual hardness tests, unless very complex experimental equipment is used in highly specialized research laboratories.

The detailed reconstruction of the point-wise thermal field of the engine, and particularly of the combustion chamber walls, is particularly important to carefully estimate local events such as surface ignitions, knock and thermo-mechanical failures (due for example to both high-cycle and low-cycle fatigue crack initiations [3][4].

The increased in-cylinder pressure in SI engines has always been limited by the arising of abnormal combustion phenomena. In particular, the autoignition of gasoline-like fuel in the periphery of the combustion chamber induces a variety of damaging mechanisms that eventually lead to severe engine failures. These include removal of the lubricant film, increasing friction and wear, and large fluctuations of the heat flux to the combustion chamber walls, affecting the high cycle fatigue strength due to thermo-mechanical loadings . Knock still remains nowadays one of the most severe performance limiters in SI engines [5][6][7][8]. Therefore, the accurate detection of the combustion chamber's knock-favorable locations allows the designers to limit the risk of abnormal combustion onset and possibly increases the specific engine performance.

As for the thermal field, the experimental analysis of the knock-prone locations is far from being trivial, and qualitative information can only be gathered through expensive in-cylinder optical visualizations or a-posteriori wear or residual hardness analyses.

In view of the limitations of the experimental practice, the need to use CAE tools, and especially CFD simulations, emerges as a fundamental step, initially for a predictive approach and later for validation and/or for problem solving [4].

In the present paper, an extensive use of such CAE methodologies is proposed. Particularly, three different simulation frameworks are used to fully reconstruct the thermal field of a high performance SI engine and carefully address its knock-related behavior. Information from each of the tools are iteratively exchanged in order to reduce the numerical uncertainties and the number of assumptions. The methodology is successfully applied to evaluate the knock tendency of the engine under its full load, peak power engine speed operation, with two different SAs.

2. Methodology

The thermal field in an internal combustion engine depends on a complex combination of many interacting factors:

- the point-wise distribution of the combustion heat fluxes on the components facing the combustion chamber;
- the effectiveness of the coolant circuit in removing heat from the most critical locations;
- the contribution (both positive and negative) by the lubricant circuit.

Temperature peaks due to local heat flux peaks and/or to inefficient heat removal could lead to mechanical failures due to the decay of the material properties and/or to the onset of abnormal combustion events such as knock and surface ignition.

As aforementioned, a numerical procedure based on mutually interacting tools is here presented to accurately reconstruct the thermal behavior of a high performance SI engine: a preliminary in-cylinder full-cycle simulation is carried out by imposing spatially averaged uniform temperatures on the combustion chamber walls in order to compute the point-wise heat flux distribution. This preliminary simulation is purposely tuned and calibrated against experimental in-cylinder pressure trace measurements.

The resulting instantaneous point-wise heat fluxes are then cycle-averaged and mapped onto the gas-exposed surfaces of a conjugate heat transfer (CHT) model of the whole engine; all the solid components and the coolant circuit are simultaneously included in the CFD model in order to account for their mutual interaction and to compute the temperature distribution within the engine under operating conditions as close as possible to the actual ones.

Thanks to the heat capacity of the solid components, in fact, the instantaneous variation of the heat fluxes during the engine cycle influences the temperature just in the very first few millimeters close to the combustion chamber walls, thus justifying the temporal, but not spatial, averaging of the heat fluxes. CHT simulations are therefore steady-state, with a resulting high reduction in computational times and costs.

The resulting temperature distribution is then used as a boundary condition for a new in-cylinder simulation. This is in fact expected to influence the evolution (both spatial and temporal) of the flame front, which in turn results in modifications to the point-wise heat fluxes acting on the surfaces. An iterative in-cylinder / CHT procedure is therefore applied [9] until negligible differences can be found between the two simulation realms and between two subsequent steps.

The above methodology is here further refined on the in-cylinder simulation side, where knock is estimated by using a tabulated approach proposed by the authors in [10].

In the modeling framework adopted in this work, the combustion chamber is considered as a two-zone region. The first one is the region where regular combustion occurs, which is treated by the ECFM-3Z combustion model. The second one is relative to the unburnt gas and the chemistry progress of the autoignition event is continuously tracked through an off-line generated map of ignition delays based on pressure, temperature, mixture strength and residual level. A purposely developed multi-linear interpolating routine is used on a cell-wise basis to accurately estimate the autoignition reaction progress, which is tracked by a passive transported precursor scalar based on the correlation by Lafossas [11]:

$$\frac{dY_{IG}}{dt} = Y_{TF} \cdot \sqrt{1 + \frac{4(1-\tau)}{\tau^2} \cdot \frac{Y_{IG}}{Y_{TF}}} \tag{1}$$

Autoignition is tracked as soon as the precursor concentration Y_{IG} locally equates the fuel tracer concentration Y_{TF}. It is then possible to define a Knock Tolerance scalar function, as the local difference between the fuel tracer and the intermediate species (2):

$$Knock\ Tolerance(\vec{x}, t) = Y_{TF}(\vec{x}, t) - Y_{IG}(\vec{x}, t) \tag{2}$$

Since knock is influenced by both the thermal state of the unburnt mixture and the spatial and temporal evolution of the flame front, modifications to the combustion chamber wall temperature distribution are expected to play a non-negligible role on the knock-occurrence probability.

The overall methodology flowchart is reported in Fig. 1 below. Since the investigated engine operation is considered as "knock-limited" by the engine manufacturer (in the sense that the imposed spark advance is the limit value to avoid potential knock damages to the engine components) a first set of calculations is performed for the experimental knock-limited spark advance (KLSA). The experimental operating condition is used to perform a preliminary qualitative validation of the methodology, and autoignition should not be verified in the integrated numerical simulations for this operation.

Then, SA is slightly advanced to promote the onset of knock-favorable locations within the combustion chamber. The iterative procedure is repeated and differences between the simplified application of spatially-averaged temperature values and CHT-derived thermal maps is highlighted.

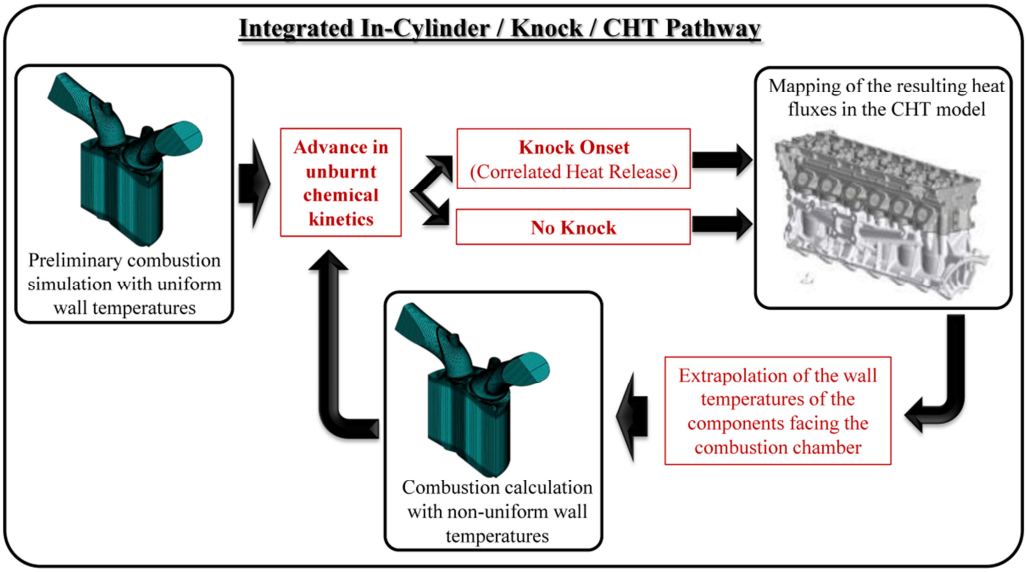

Fig. 1. Interaction between in-cylinder and CHT simulations.

3. The engine

The studied engine is a 12 cylinder V-shaped direct injection spark ignition (DISI) naturally aspirated engine, whose characteristics are reported in the Table 1 below.

Table 1. Engine parameters

Displacement	≈ 6300 cm^3
Bore/Stroke Ratio	> 1.1
Max Power	> 540 kW @ 8000rpm

The investigated operating point is the 7500rpm WOT full load/peak power one. The SA is the KLSA one for this condition; however the exact value cannot be indicated for confidentiality issues.

4. CFD Simulations

In-cylinder and CHT simulations are performed in different frameworks, and their mutual interaction is carried out through a mapping procedure of the calculated quantities of interest from one simulation realm to the other. Those quantities, mainly consisting of temperatures, heat fluxes and heat transfer coefficients (HTC), are used as boundary conditions, thus making possible an iterative exchange of information from the single in-cylinder simulation to the complete engine CHT one and vice-versa.

In the next paragraphs, the computational domain and the numerical setup for both the simulations are detailed.

4.1 In-cylinder simulations

The combustion analyses are developed in the framework of Star-CD 4.18 licensed by CD-adapco. The combustion model adopted for the analyses is the ECFM-3Z, whose well-known suitability for premixed as well as diffusive and autoigniting combustion regimes is a fundamental requirement for the present study. In particular, knock is taken into account thanks to a hybrid user-coded/standard formulation which was previously described and is hereafter further commented. First, the chemical kinetics progress towards autoignition is calculated in the unburnt mixture based on a autoignition delay interpolating routine internally developed at University of Modena and widely described in [10]. Detailed autoignition results from a constant pressure reactor are calculated over a wide range of in-cylinder conditions of pressure, temperature, mixture strength and residuals by means of DARS-Basic software [12] and based on a semi-detailed chemical mechanism for a RON98 European gasoline provided by the fuel supplier [13]. The fuel is injected by means of a 7-hole injector placed between the intake valves. The two-phase flow modeling is carried out by means of a user coded routine for primary breakup, the Reitz model for secondary break-up and the Bai-Gosman approach for droplet-wall interaction. Due to the very early injection time, liquid film can be a major contribution to both heat removal from the walls (especially from the piston) and spray mixing. To this aim, liquid film formation is considered in the CFD simulation.

In order to achieve a converged solution, several RANS cycles were performed based on periodic boundary conditions for the analyzed cylinder, derived from a 1D model of the whole engine provided by the engine manufacturer. Once a cyclic-converged cycle is obtained, this represents the baseline for the subsequent analyses.

As far as wall temperatures are concerned, uniform wall temperatures derived from literature are applied for the first simulation. In particular, wall temperatures are: 473 K at the dome, 540 K at the piston crown, 410 K at the cylinder liner, 640 K at the intake valve face and 950 K at the exhaust valve face. As the in-cylinder / CHT loop is performed and mapped wall temperatures are calculated, the same combustion simulation is repeated with the new surface thermal field distribution. The knock tendency and its variation with the wall temperature field is then evaluated. Thanks to the symmetry of the geometry just half a model is considered for the in-cylinder simulations.

4.2 Conjugate heat transfer simulations

In order to properly estimate the effectiveness of the cooling circuit, the accurate representation of the fluid/solid interaction is of primary importance: in CHT analyses both the coolant and the metal components are modeled together. Information between the two domains are exchanged through interfaces. The same is done for solid/solid contact regions.

Thanks to the V-shaped architecture of the engine, just one solid bank is considered, in order to save computational resources, while the coolant circuit is fully included because of the specific circuit architecture to prevent numerical instability at the bank inlet; still, just a half of the cooling jacket is surrounded by the metal components and plays an active role in the CHT analysis and heat removal process. On the solid side, the calculation domain includes the engine head, the engine block, the gasket, valve seats and guides, intake and exhaust valves and a simplified model of the spark plug. The piston is separately analyzed: the steady-state approach for the CHT simulation, thanks to the high thermal inertia of the engine components, prevents to include the piston itself in the computational domain since, because of its motion during the engine cycle, any arbitrarily imposed position would affect the point-wise thermal distribution at the liner/piston interface. As a consequence, a separate piston model is created considering the effects of the cycle-averaged point-wise thermal fluxes due to combustion on the piston

crown, the interaction with the lubricant, with the rings and with the pin, these last contributions being modeled as a network of thermal resistances. A detailed description can be found in [9]. The resulting heat transfer from the piston to the liner is added to the quantity due to the sole combustion process, and the total amount is applied by a proper polynomial function over the cylinder liners in the CHT model. Even if the valves are in motion during the engine operations, they are assumed to be in their closed position, and the heat transfer from/to the valve seats and guides is mimicked by a proper contact resistance, in order to consider the lack of contact during a portion of the engine cycle. A further thermal resistance is applied to all the interfaces (that are green colored in Fig. 2a) between two adjacent solid components, whose value depends on contact pressure and material properties.

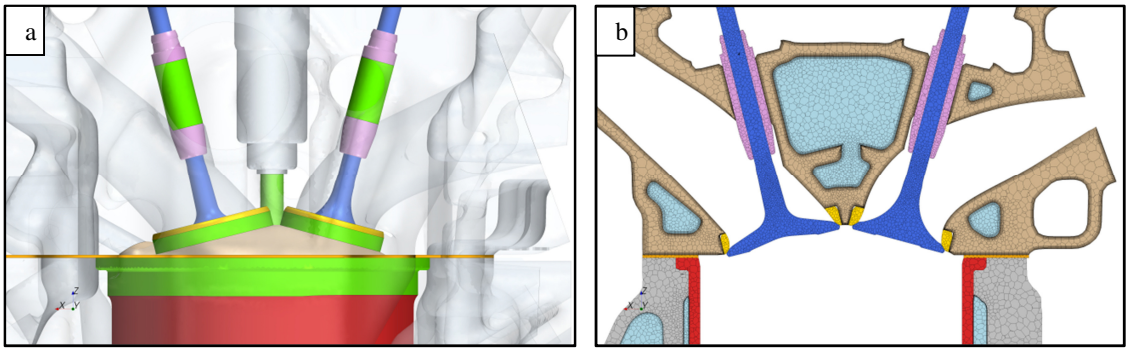

Fig. 2. (a) Solid components and their common interfaces; (b) mesh of the calculation domain.

The computational mesh is represented in Fig. 2b: on the fluid side, it is based on a polyhedral core mesh with 5 prismatic layers for the calculation of the boundary layer (according to the all-y+ wall treatment); on the solid side, a polyhedral core mesh is used too, while a prismatic multi-layer mesh is adopted for the solid walls only if the thermal conductivity dependency with temperature is available, in order to improve the estimation of the thermal boundary layer gradients in the metal components.

5. Numerical Validation With Experimental Data

The first part of the study deals with the validation of the in-cylinder CFD full-cycle simulation results against the ensemble average experimental pressure trace. The spark advance adopted in the simulation is the same as the one indicated by the experiments as the knock limited one. To this aim, uniform wall temperatures are imposed in the in-cylinder CFD analysis (hereafter named InCyl-0). The validation is reported in Fig. 3 below.

Once the overall combustion behavior is satisfactory, the resulting point-wise / cycle-averaged heat flux distribution derived from the InCyl-0 simulation is mapped into the CHT model, named CHT-0; a first thermal field of the entire engine is then calculated. The computed wall temperatures of the components facing the combustion chamber are then used as a boundary condition for a new in-cylinder simulation, called InCyl-1, and this loop is performed until the convergence is met. In order to draw a proper comparison between the in-cylinder runs, the same initial conditions are used, being the wall thermal field the only variation among the in-cylinder evaluations.

The wall temperature difference between InCyl-1 and InCyl-0 is shown in Fig. 4 hereafter. It is evident that the temperature field is largely non-uniform, and this is expected to influence both the flame front behavior and the point-wise knock tolerance index distribution. The combustion dome exhibits a higher temperature on the exhaust side, while the exhaust valves are not so far from the initial uniform temperature. Intake valves, instead, are far from the commonly adopted boundary conditions, and the local temperature peak can exceed the uniform reference value by 150K.

As far as knock tendency is concerned, an immediate observation is that a large difference in Knock Tolerance can be observed for the valve face regions, due to the relevant difference in the thermal field distribution resulting from the in-cylinder / CHT loop. This is reported in Fig. 4c. In particular, the mapped thermal field case exhibits a higher knock resistance in the outer exhaust valve region (red colored areas), due to the slightly lower valve

temperature with respect to the uniform one. Conversely, the intake valve region shows a reduction in knock safety (blue colored regions) as a straightforward consequence of the hotter surfaces, which were strongly underestimated by using uniform wall temperatures.

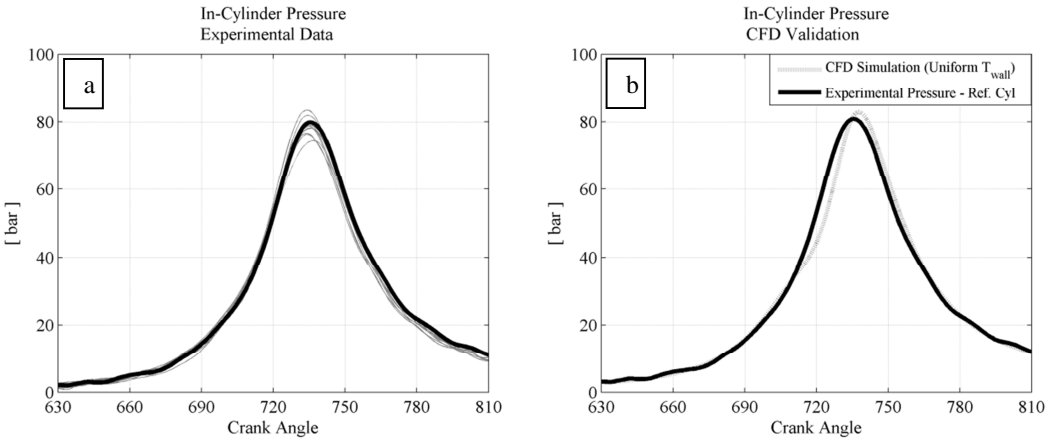

Fig 3. (a) Cylinder-specific ensemble average pressure trace (thin grey lines); reference cylinder is highlighted (thick black line). (b) CFD pressure trace against experimental data for reference cylinder.

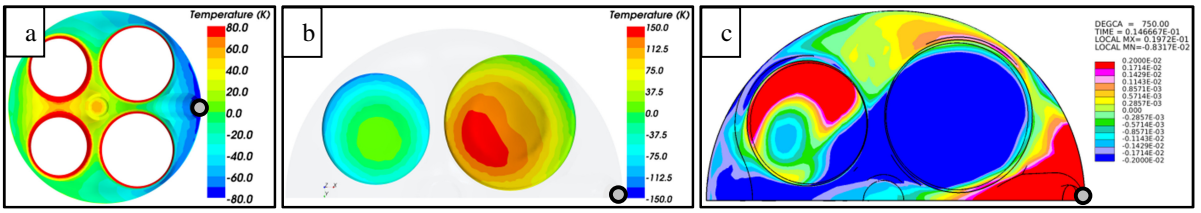

Fig. 4. (a) Dome wall temperature difference between InCyl-1 and InCyl-0; (b) the same difference for the valve faces; (c) difference of Knock Tolerance at +30CA aTDC between InCyl-1 and InCyl-0. In all figures the probe is reported as a gray dot.

InCyl-0 calculation shows that the most critical portions of the combustion chamber in terms of knock are the outer region of the exhaust valves seats and the injector cavity. The InCyl-1 simulation, thanks to the point-wise temperature distribution, exhibits a reduction in the knock safety for the outer exhaust seats regions, while the injector cavity area strongly benefits from the reduced local temperature.

In order to assess the improvement in the local reaction rate brought by the mapped wall thermal distribution, a closer insight is performed in these areas based on local probe measurements reported in Fig. 5, whose location is illustrated in Fig. 4. The local analysis provided by the injector-close gauge measures a largely reduced unburnt gas overheating. This is particularly significant as this is the most knock-prone region in the whole combustion chamber. As the knock onset is a locally-driven phenomenon, in this case the point-wise temperature distribution derived from the in-cylinder / CHT loop allows to assess a larger tolerance before knock onset than the uniform wall temperature calculation.

In Fig. 6, the combustion pressure traces as well as the burn rates are reported for InCyl-0 and InCyl-1 cases. In order to reach a better matching with the experimental data, a slight tuning of the ignition parameters is performed: in fact the flame front evolution is influenced by the temperature field distribution and a combustion validation based solely on uniform wall temperature analysis would have been intrinsically wrong. A first validation of the KLSA condition indicated by the experiments is the absence of heat release due to autoignition for all the in-cylinder / CHT iterations. This is confirmed by the scatter plot representation reported in Fig. 6c, where all the unburnt fluid cells in a late combustion CA are located in the knock-free region.

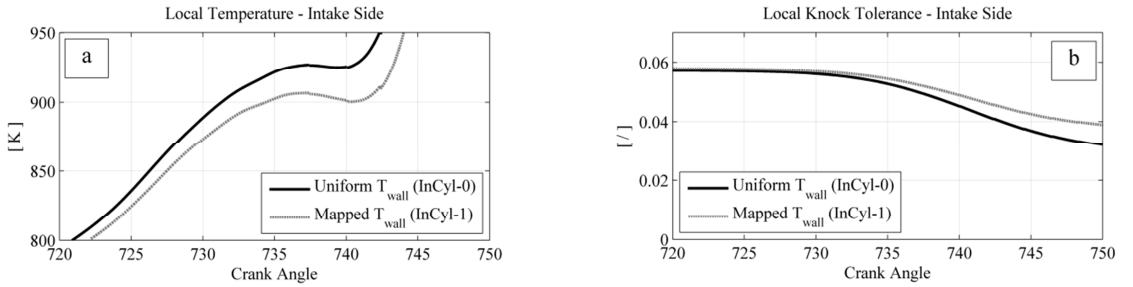

Fig. 5. (a) Local temperature measured by the probe close to the injector location, for both the InCyl-0 and the InCyl-1 cases. (b) Knock Tolerance for the same location in both cases.

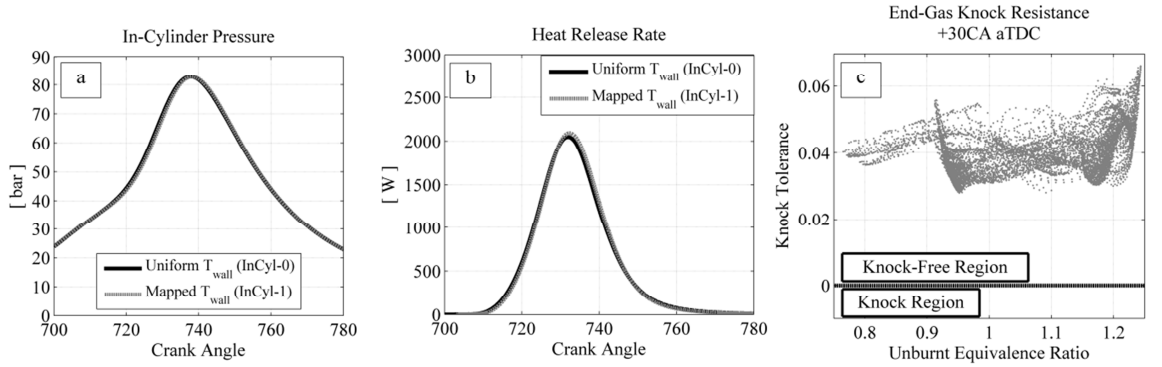

Fig. 6. (a) In-cylinder CFD results from the in-cylinder / CHT loop; (b) Heat release rate from CFD results; (c) Knock Tolerance scatter plot at +30CA aTDC.

6. Combustion and Knock Tendency Results for Advanced Spark Timings

In order to fully validate the KLSA condition indicated by the experiments, and confirmed as knock-safe in the previous section, a discrete increase of the SA is now evaluated. A new set of in-cylinder / CHT simulations is run by advancing the experimental spark timing by 3 CA (KLSA+3). The same loop as above is performed, starting from uniform wall temperatures and adopting the same initial condition for all the thermal field distribution at solid walls. The combustion results for the increased SA are reported in Fig. 7, together with the heat release rate and the Knock Tolerance scatter plot, where the same CA as the one in Fig. 6c is used. As can be seen from Fig. 7b, at 750CA heat release fluctuations due to knock are present.

The faster burn rate for the mapped thermal field case is evident for the considered SA. This triggers the knocking event earlier in the cycle and a larger mass of unburnt mixture is involved in it; thus, a higher knock intensity is experienced, depicted by the impulsive heat release at the combustion tail visible in Fig. 7b.

In Fig. 8 the net variation in the wall heat flux due to the increased SA is reported, for both the dome and the valve faces. A growth in the wall heat flux is observed in the spark plug region and in the adjacent valve seat and face portions. This is due to the advanced combustion phasing. On the other hand, a significant increase in the thermal flux is measured in the injector cavity region, and this is due to autoignition. This is in agreement with the observation from the previous section, which indicated this as the most knock-prone region. The KLSA+3 condition is sufficient to trigger the arise of knock onset, as it is visible in Fig. 9a.

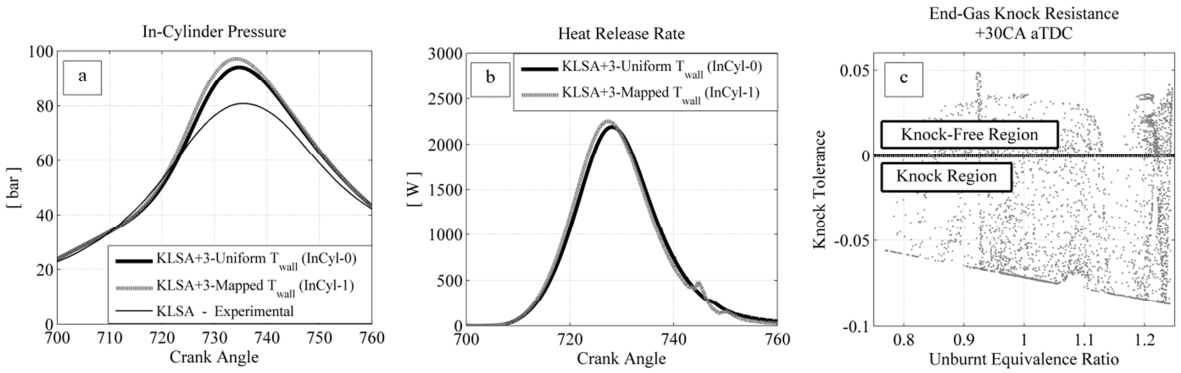

Fig. 7. (a) In-cylinder pressure for KLSA+3 case, experimental KLSA pressure trace is reported as a reference; (b) Heat release rate for KLSA+3; (c) Knock Tolerance scatter plot at +30CA aTDC.

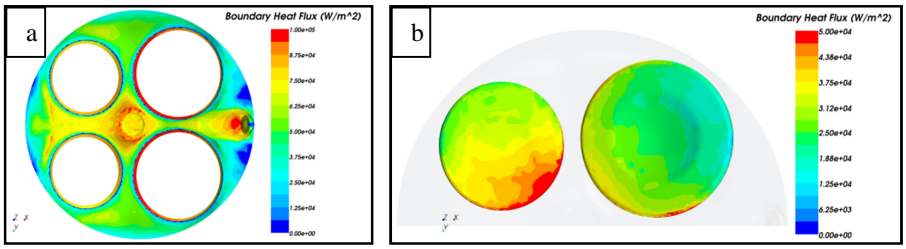

Fig. 8. Net wall heat flux variation from the KLSA to the increased one (a) on the cylinder dome and (b) on the valves.

In Fig. 9 the cumulative heat released by autoignition is reported at +30CA aTDC, for both the InCyl-0 and InCyl-1 case. The relative advance in the knocking event is evident for the latter case. These results depict from a numerical point of view the well-known self-enforcing feature of knocking combustion. It is well acknowledged that the impulsive heat release close to the solid walls induces a set of sonic pressure waves which originate a variety of damaging effects. One of the most important is the removal of the thermal boundary layer adjacent to the metal components due to the reflecting pressure pulse: this in turn causes an abnormal increase in the thermal flux to the solid walls, thus, combustion chamber wall HTC peaks are experienced. This unbalances the thermal budget of the combustion chamber towards a larger heat loss.

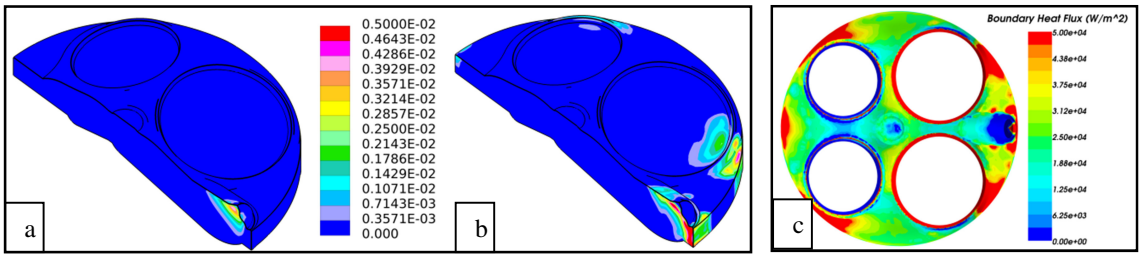

Fig. 9. Heat released by autoignition for KLSA+3 case. (a) InCyl-0 case. (b) InCyl-1 case; (c) heat flux variation for KLSA+3 between InCyl1 and InCyl-0.

The higher wall temperature that is imposed for the following in-cylinder / CHT loop (in the experimental practice in the following engine cycle) induces a higher reaction rate for the adjacent unburnt charge, thus anticipating the knocking event and leading to a self-enforcing damaging mechanism.

7. Conclusions

This study is the prosecution and integration of two different research topics formerly carried out independently by the authors. In particular, a previously developed in-cylinder / CHT methodology is combined with a look-up table approach for knock prediction. The different frameworks interact through the exchange of thermal boundary conditions. The integrated methodology is applied on a production GDI engine and is validated with reference to experimental knock-limited data.

This activity confirms the sensitivity of the combustion and knock prediction calculations on the thermal boundary conditions. In particular, a point-wise temperature distribution derived from CHT simulations of the whole engine modifies the overall burn rate and, in particular, the location of the critical hot spots in the combustion chamber, i.e. those where knock is most probable to arise. Even in a knock-safe condition, indicated by the experimental test bed, the knock proximity entity and distribution largely varies going from a uniform wall temperature distribution to a mapped one. If knock is not present, the in-cylinder / CHT loop leads to a convergence in terms of heat fluxes due to the combustion and thermal field in the CHT model. This is verified for the experimental KLSA and constitutes a first validation of the methodology. On the contrary, if knock is present the self-enforcing feature of the phenomenon is captured by the in-cylinder / CHT loop. This is significant nevertheless the steady state approach adopted in CHT model. This is shown by increasing the KLSA by 3 CA, thus moving the operating point out of the knock-safe range. The in-cylinder / CHT loop shows a progressively increase in wall temperature due to the heat release by knock, and this in turns leads to an earlier and more intense autoignition event in the following iteration. Moreover, the location of the hot spots is influenced by the wall thermal results from the CHT simulation. As a final consideration, from the obtained results an erroneous knock onset prediction due to the application of the simplified thermal boundary conditions emerges as a potential mistake. This would introduce an improper heat release in the in-cylinder / CHT loop, that would badly affect the subsequent iterations.

References

[1] Turner JWG, Pearson RJ, Kenchington SA. Concepts for improved fuel economy from gasoline engines. *International Journal of Engine Research*; January 1, 2005, vol. 6, 2, pp. 137-157.

[2] Fraser N, Blaxill H, Lumsden G, Bassett M. Challenges for Increased Efficiency through Gasoline Engine Downsizing. *SAE Int. Journal of . Engines 2(1)*; 991-1008, 2009, doi:10.4271/2009-01-1053.

[3] Plengsaard C, Rutland C. Improved Engine Wall Models for Large Eddy Simulation (LES). *SAE Technical Paper 2013-01-1097*; 2013.

[4] Fontanesi S, Giacopini M. Multiphase CFD–CHT optimization of the cooling jacket and FEM analysis of the engine head of a V6 diesel engine. *Applied Thermal Engineering*; Volume 52, Issue 2, 15 April 2013, Pages 293-303, ISSN 1359-4311, http://dx.doi.org/10.1016/j.applthermaleng.2012.12.005.

[5] Dahnz C, Spicher U. Irregular combustion in supercharged spark ignition engines: Pre-ignition and other phenomena. *International Journal of Engine Research*. 2010(11), 485-498.

[6] Kalghatgi GT, Bradley D. Pre-ignition and 'super-knock' in turbocharged spark-ignition engines. *International Journal of Engine Research*. August 2012, vol. 13 no. 4, 399-414.

[7] Kawahara N, Tomita E, Sakata Y. Auto-ignited kernels during knocking combustion in a spark-ignition engine. *Proceedings of the Combustion Institute*. Volume 31, Issue 2, January 2007, Pages 2999-3006, ISSN 1540-7489, http://dx.doi.org/10.1016/j.proci.2006.07.210.

[8] Kleemann A, Menegazzi P, Henriot S, Marchal A. Numerical Study on Knock for an SI Engine by Thermally Coupling Combustion Chamber and Cooling Circuit Simulations. *SAE Technical Paper 2003-01-0563*, 2003, doi:10.4271/2003-01-0563.

[9] Fontanesi S, Cicalese G, Tiberi A. Combined In-cylinder / CHT Analyses for the Accurate Estimation of the Thermal Flow Field of a High Performance Engine for Sport Car Applications. *SAE Technical Paper 2013-01-1088*, 2013, doi:10.4271/2013-01-1088.

[10] Fontanesi S, Paltrinieri S, D'Adamo A, Cantore G et al. Knock Tendency Prediction in a High Performance Engine Using LES and Tabulated Chemistry. *SAE Int. J. Fuels Lubr*. 6(1):98-118, 2013, doi:10.4271/2013-01-1082.

[11] Lafossas FA, Castagne M, Dumas JP, Henriot S. Development and Validation of a Knock Model in Spark Ignition Engines using a CFD code. *SAE Technical Paper 2002-01-2701*; 2002.

[12] DARS Manual Book 2 – Homogeneous Reactor Models.

[13] Andrae JCG, Head RA. HCCI Experiments with gasoline surrogate fuels modeled by a semidetailed chemical kinetic model. *Combustion and Flame* 156; 2009, 842-851.